Enzyme-Targeted Fluorescent Imaging Probes on a Multiple Antigenic Peptide Core

Amit K. Galande, Scott A. Hilderbrand, Ralph Weissleder, and Ching-Hsuan Tung*

Center for Molecular Imaging Research, Massachusetts General Hospital, Harvard Medical School, Charlestown, Massachusetts 02129

Received October 6, 2005

Peptide dendrimers have a variety of applications in biology such as the vehicles for drug and gene delivery, molecular inhibitors, protein mimics, and synthetic vaccines. The multiple antigenic peptide (MAP) system is a well-known example of a discrete, dendrimeric scaffold. We explored a novel application of the MAP-based scaffold by designing molecular probes that fluoresce only after enzymatic treatment. The probes, which were synthesized on solid support, incorporate a cathepsin S dipeptide substrate (Leu-Arg), and a poly(ethylene glycol) (PEG) chain in their dendritic arms. The fluorescence emission of the near-infrared fluorochromes attached to the N-termini of the dendritic arms was quenched. Mechanistic studies revealed formation of H-type dye aggregates within the tetravalent MAP system. By varying the length of the PEG chain, three probes were synthesized, CyPEG-1, CyPEG-2, and CyPEG-3 with 4, 8, and 12 ethylene oxide units, respectively. CyPEG-2 showed optimum aqueous solubility and quenching efficiency for imaging applications. Upon proteolytic activation with cathepsin S (EC 3.4.22.27), CyPEG-2 showed greater than 70-fold increase and more than 95% recovery in fluorescence emission.

Introduction

Targeted fluorescent probes are valuable tools in molecular imaging.[1] Their efficiency as imaging agents can be improved if their fluorescence emission can be turned on only at the target site. Equally important, enzyme targeting can be used to reveal tissue specific molecular information by imaging. One strategy for the design of such probes is by incorporation of a molecular switch where the fluorochromes in the probe are quenched efficiently. A variety of peptidic,[2] polymeric,[3] and nanospheric[4] scaffolds have been used to conjugate fluorescent dyes. Macromolecular polymer- and nanosphere-based systems have been shown to work exceedingly well because they provide a platform for efficient quenching and can be delivered readily to tumors because of the enhanced permeability and retention (EPR) effect.[5] Such macromolecular systems, however, have certain drawbacks, which we attempted to circumvent in this research. First is the variability in the size of the scaffold. Most polymer- or nanosphere-based systems have polydispersity and heterogeneity associated with them, making precise characterization of the probe difficult or ambiguous. Second, neither the specific site nor the extent of conjugation, such as pegylation or fluorochrome attachment, can be easily controlled in such systems. Finally, some of these macromolecular probes may be retained in nontargeted tissues for extended periods of time due to their long circulation time, and slow blood clearance.

Peptide-based probes have the potential to eliminate these drawbacks. Well-established solid-phase synthetic methods[6] allow custom synthesis of reproducible constructs with defined chemical structure and molecular mass. Hence it is desirable to make discrete peptide-based probes that are smaller, thus facilitating their rapid clearance and precise characterization.

The multiple antigenic peptide (MAP) system[7] is a well-known example of a small and discrete, dendrimeric scaffold. This system has been used extensively in a variety of biomedical applications such as for the vehicles of drug and gene delivery, molecular inhibitors, protein mimics, and synthetic vaccines.[8] It has been observed that peptides making the dendritic arms of the MAP system have a tendency to aggregate.[7] Hence we hypothesized that it would be possible to quench fluorophores by aggregation if they are attached to the termini of the dendritic arms of the MAP system. The quenched probe could then be targeted to the enzymes of interest by incorporating the corresponding peptide substrate in the dendritic arms. The probe is expected to fluoresce after activation by the enzymatic cleavage of the peptide bond. This strategy of making enzyme sensitive probes is depicted in Figure 1, and as a proof-of-principle, herein we describe solid-phase synthesis, characterization, and evaluation of peptide-based cathepsin S activatable probes.

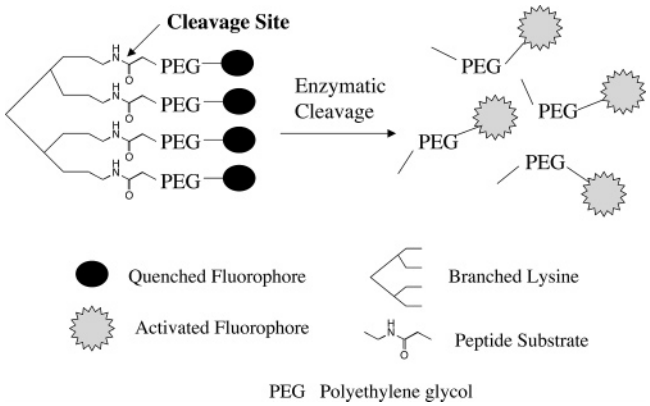

Figure 1. Design of a fluorescent probe with a molecular switch on a multiple antigenic peptide (MAP) core.

Results and Discussion

Design of the Probes. The synthetic scheme and molecular structures of the probes are given in Figure 2. The probes are based on a tetravalent, branched lysine core. Extending from the core are the dendritic arms that incorporate a dipeptide, Leu-Arg, as a substrate[9,10] for the targeted protease, cathepsin S. To facilitate the interaction of the peptide substrate with the active site of the enzyme, we attached β-alanine as a spacer molecule on the either side of the peptide substrate. To the four N-termini of this peptidic scaffold we attached CyTE-777, a near-infrared

* To whom correspondence should be addressed. Tel: 617-726-5779. Fax: 617-726-5708. E-mail: tung@helix.mgh.harvard.edu.

10.1021/jm051001a CCC: $33.50
Published on Web 07/01/2006

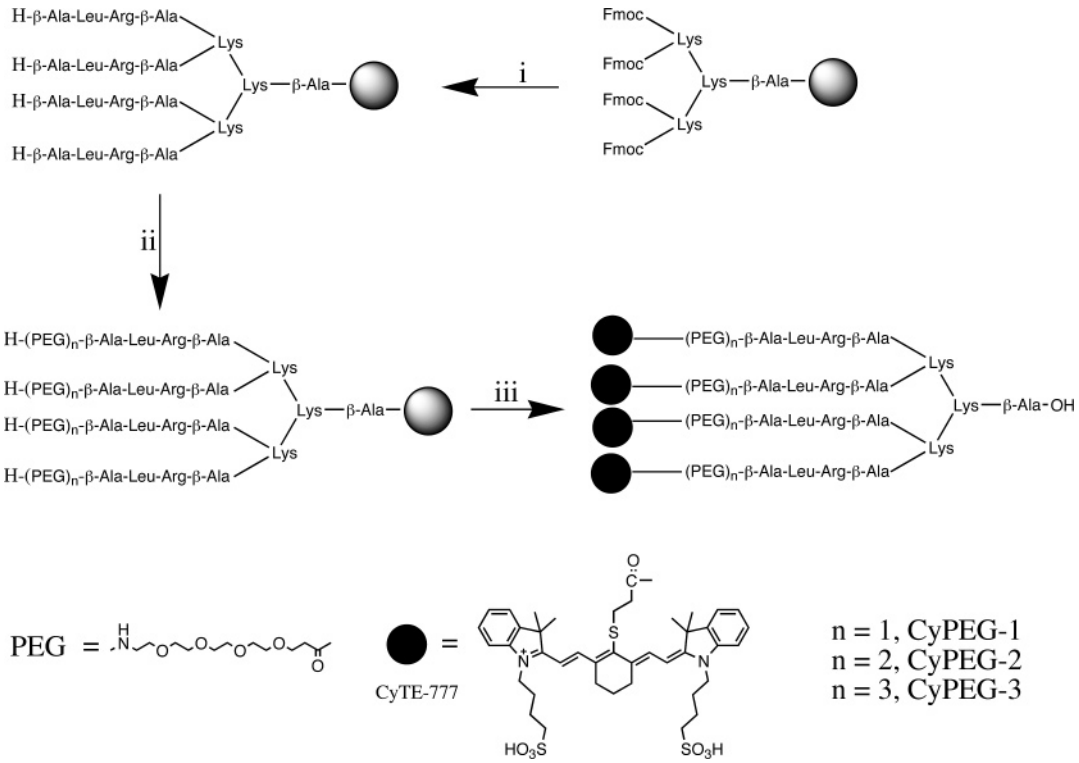

Figure 2. Solid-phase synthesis and molecular structures of MAP-based fluorescent probes; conditions: (i) 20% piperidine in DMF, Fmoc-amino acid-OH, HBTU/HOBt/DIEPA in DMF, (ii) Fmoc-15-amino-4,7,10,13-tetraoxapentadecanoic acid/PyBOP/DIEPA in 9:1 NMP/DCM, 20% piperidine in DMF, (iii) CyTE-777, DCC/HOBt in anhydrous DMF, TFA/TIS.

fluorescent dye.[11] The fluorochrome contains a central carboxylic acid for conjugation to biomolecules, has absorption (777 nm) and emission (812 nm) bands similar to indocyanine green, and shows no tendency to aggregate in aqueous media.

Because of the branched lysine core, however, aggregation of the dye molecules within the probe is expected. While dye aggregation provides efficient quenching, it invariably results in decreased aqueous solubility. To optimize the aqueous solubility of the probes, short and discrete poly(ethylene glycol) (PEG) moieties were inserted between the fluorophores and the peptides. PEG has a dynamic conformation and is well hydrated in aqueous media, which results in improved aqueous solubility of a pegylated molecule.[12] However, this property of PEG can be counterproductive for the design of a quenched probe because the PEG chain may help disrupt the hydrophobic interactions between the dye molecules, leading to inefficient fluorescence quenching. PEG was incorporated in the dendritic arms to achieve balance between the dye aggregation and the aqueous solubility of the probe. Hence, at the onset, it was required to determine the optimum PEG chain length that can improve the aqueous solubility of the probe but at the same time does not weaken dye aggregation. Accordingly, a series of probes with four (CyPEG-1), eight (CyPEG-2), and twelve (CyPEG-3) ethylene oxide units in the dendritic arms were synthesized (Figure 2). The bifunctional PEG chain utilized in this design has no polydispersity. Thus, each probe is a single chemical entity. Homogeneity of the probes was confirmed using RP-HPLC (Figure 3), and their masses were confirmed using ESI-MS (Table 1).

Wavelengths (λ_{max}) of fluorescence excitation and emission of CyTE-777 did not change after its conjugation to the dendritic scaffold. Successful synthesis of these probes demonstrates utility of CyTE-777 in solid-phase synthesis. On-resin synthesis typically requires excess of reagents to drive the reactions to completion. Most commercially available cyanine dyes are impractical for solid-phase synthesis considering their high cost and poor stability in strong acidic and basic conditions. CyTE-777 affords access to a variety of constructs for in vivo imaging based on solid-phase synthesis.

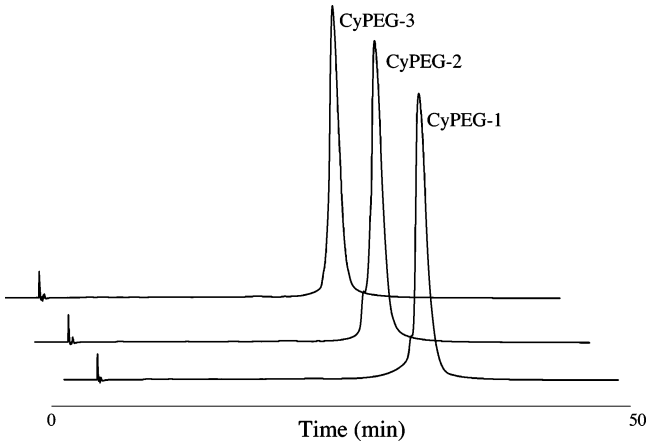

Figure 3. HPLC traces of the purified samples of probes CyPEG-1, CyPEG-2, and CyPEG-3.

Table 1. Characterization Data for CyPEG-1, CyPEG-2, and CyPEG-3

probe	mol. mass (calc)[a] (Da)	mol. mass (found)[b] (Da)	retention time[c] (min)
CyPEG-1	6224.1	6225.6	31.99
CyPEG-2	7212.7	7213.2	30.63
CyPEG-3	8201.2	8201.5	29.46

[a] Theoretical molecular mass expected for the molecular ion M^+. [b] Molecular mass found from the ESI-MS for the molecular ion M^+ ionic species. [c] See the Experimental Section for details of the conditions used in the RP-HPLC.

Quenching Studies. The absorption spectra of equimolar solutions of the probes based on the absorption peak of the free dye, CyTE-777, are shown in Figure 4. A new peak at 705 nm,

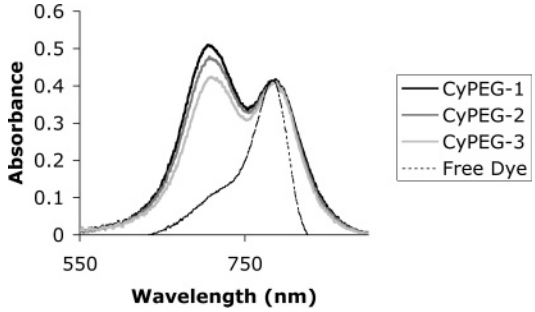

Figure 4. Absorption spectra: effect of pegylation on dye aggregation of the probes. The aggregation of dyes was seen as a strong absorption at around 705 nm.

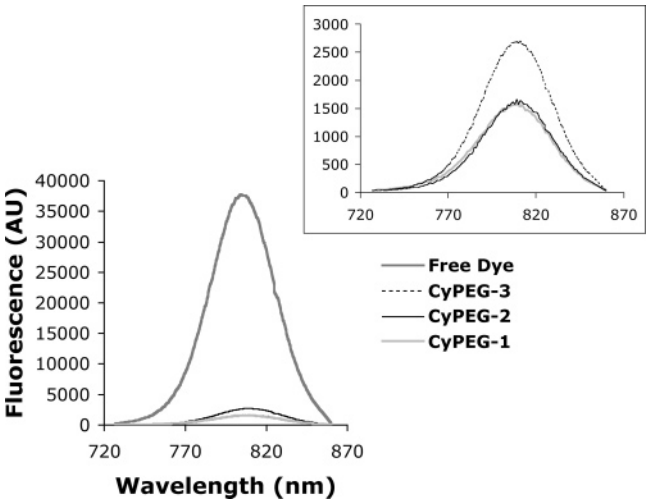

Figure 5. Fluorescence spectra of ~3 μM solutions (20% DMSO in 10 mM phosphate buffer, pH 7.4) of the probes compared with an equimolar solution of CyTE-777; excitation wavelength 750 nm. The insert is the expanded region of fluorescence spectra for CyPEG 1−3.

which is blue-shifted by about 80 nm from the absorption peak of the free dye was observed for all the three probes indicating dye aggregation. At this concentration (3 μM), free CyTE-777 does not show any aggregation in water or aqueous buffered solutions. However, after its conjugation to the branched lysine core, the probe displays significant dye aggregation thus demonstrating the ability of the branched lysine scaffold to promote aggregation. The absorption band due to dye aggregation becomes slightly weaker with increasing PEG chain length. CyPEG-1, with the strongest dye−dye aggregation, is practically insoluble in aqueous solutions. CyPEG-2 and CyPEG-3, on the other hand, showed satisfactory aqueous solubility. To determine if the aggregated fluorophores lead to quenching, fluorescence spectra of all the three probes were measured and compared to the fluorescence spectrum of an equimolar solution of CyTE-777 (Figure 5). All the probes displayed superior quenching efficiency with CyPEG-1 (95.6%) and CyPEG-2 (95.6%) showing better quenching than CyPEG-3 (92.3%).

Mechanism of Quenching. Typically, in a homolabeled probe, two possible mechanisms are suggested to explain the quenching phenomenon. First is the fluorescence resonance energy transfer (FRET), based on a weak dipole−dipole interaction, and second is static quenching, based on strong dipole−dipole interactions, where the fluorochromes form nonfluorescent ground-state complexes.[13] In FRET-based quenching, the fluorophore and quencher molecules retain their intrinsic properties such as the absorption spectrum. Static quenching, however, is associated commonly with significant changes in the absorption spectra. If the interaction between the two dyes leads to a new blue-shifted absorption maximum, then the type of association is termed H-dimer, an alignment between the two dyes such that a radius vector connecting the two chromophores is perpendicular to their transition dipoles.[13] Such association typically produces weakly fluorescent complexes with their own distinct absorption spectra. In homodimers it is possible for an H-type aggregate to have no fluorescence because identical transition dipoles are coupled which can completely cancel each other if properly aligned.[13] In such a dimeric state, absorption and emission of light are by the dimeric unit.

This mechanism is quite different from the FRET. In a heterolabeled probe, the spectral overlap between a donor and an acceptor gives rise to absorption of light by the donor chromophore, resonance energy transfer to the acceptor chromophore, and emission with the spectral characteristics of the acceptor exclusively. In a homolabeled probe, however, each chromophore has a dual role of being a donor as well as an acceptor.

H-dimers typically have diminished fluorescence, and as indicated in Figure 4 all the probes showed substantial decrease in fluorescence as compared to their free dye counterpart at the same concentration. As indicated in Figure 4, the absorption spectra of all the three probes showed a substantial aggregation peak (705 nm). Formation of H-dimers, confirmed by the absorption and fluorescence spectra, suggest static quenching of CyTE-777 in the probes.

However, FRET-based quenching of the fluorophore is also feasible because CyTE-777 has a relatively small Stoke's shift (~30 nm).[11] The small Stoke's shift results in significant overlap between the absorption and the emission spectra of CyTE-777. This overlap facilitates FRET and subsequent quenching of the fluorophore. FRET typically occurs over distances up to 20−60 Å. In a MAP-based system, the dye molecules are in close association with each other, and FRET is expected for the molecules that do not form H-dimeric complexes. Thus, in the MAP-based design of a fluorescent quenched probe, the contribution from the FRET-based quenching of the probe cannot be ruled out.

To investigate the contribution of FRET to the quenching of the probe, the dye−dye aggregation and static quenching mechanisms were eliminated by alteration of the solvent polarity. Equimolar solutions (6.5 μM) were made for CyPEG-1 and CyTE-777, and the absorption spectra and fluorescence quenching of CyPEG-1 were monitored and compared to the free dye in 20% and 99% DMSO (Figure 6). As compared to free CyTE-777, the blue-shifted aggregation peak of CyPEG-1 observed in 20% DMSO can be entirely eliminated by dissolving the probe in 99% DMSO. Thus, in 99% DMSO, there is little or no contribution from formation of nonfluorescent ground-state complexes on the quenching of CyPEG-1. To evaluate the contribution of FRET on the quenching of CyPEG-1, we measured fluorescence of CyTE-777 and CyPEG-1 in 20% DMSO and 99% DMSO. In 20% DMSO, the fluorescence emission of the free dye is approximately 38-fold greater than that observed for CyPEG-1. In 99% DMSO, where there is negligible contribution from static quenching in CyPEG-1, the fluorescence emission from the free dye is only 1.7 times that of CyPEG-1 indicating static quenching as the predominant mechanism in the MAP-based system of the probes.

Probes based on static quenching represent a significant advantage over FRET-based probes because in homolabeled probes where static quenching mechanism predominates, an

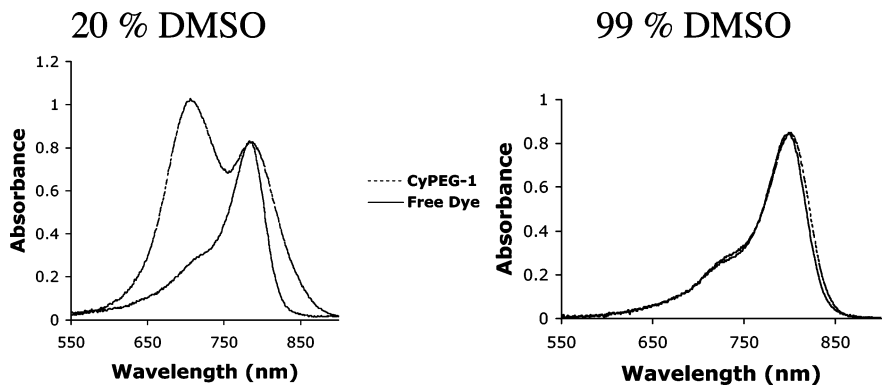

Figure 6. Mechanistic studies: a strong aggregation peak (705 nm) observed in 20% DMSO is absent in 99% DMSO.

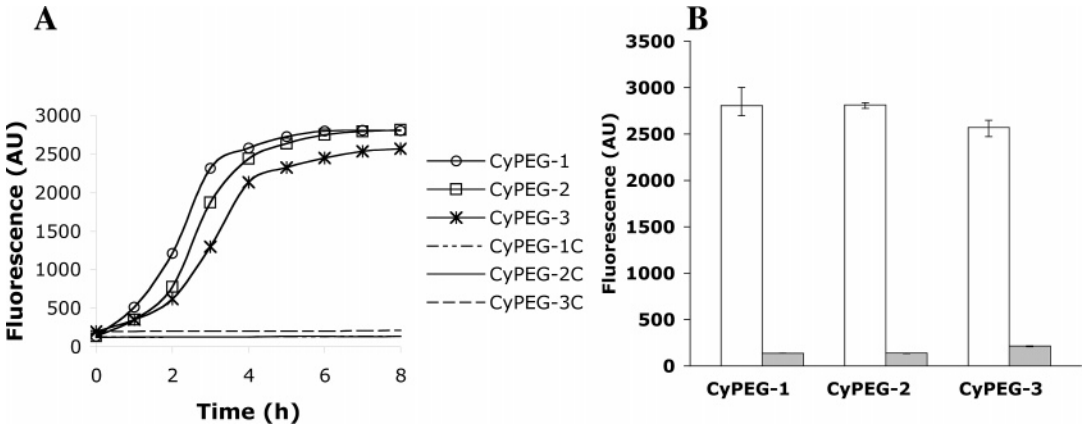

Figure 7. (A) Effect of pegylation on the kinetic profile of the probe activation with cathepsin S in 20% DMSO solution of pH 7.4, as compared to the controls (no enzyme added) CyPEG-1C, CyPEG-2C, and CyPEG-3C. (B) Probe activation (open bar) after 8 h at 810 nm as compared to the non-cathepsin S controls (solid bar). The results are means ± SD of three independent experiments.

intrinsically more favorable signal-to-noise ratio is obtained in which the signal itself is truly fluorogenic.[13]

Enzymatic Studies. Considering the differential solubility of the probes, the enzyme activation studies were conducted in the presence of 20% DMSO in 10 mM phosphate buffer solution of pH 7.4. As expected, all the probes showed an increase in fluorescence on treatment with cathepsin S (Figure 7). Enzymatic activation, caused by the proteolytic release of the fluorochromes, slowed with increase in the length of the PEG chain. After 8 h, fluorescence from all the probes reached saturation. Fluorescence obtained at this time point was compared to the fluorescence of control where no enzyme was added. Of the three probes, CyPEG-3 displayed the smallest increase in fluorescence signal. This can be attributed to its longer PEG chain length, which results in weaker dye−dye aggregation and therefore a higher fluorescence background.

The increase in fluorescence as compared to the background signal is an important factor when evaluating the efficiency of an enzyme activatable probe. Another criterion for the evaluation of the probes is the fluorescence recovery after activation, which is determined by comparing the fluorescence signal of an activated probe after complete enzymatic degradation, with the fluorescence from an equimolar solution of the free fluorochrome. In our studies, all the three probes showed greater than 95% recovery of fluorescence.

In a separate experiment, the probe activation was studied in the presence of serum proteins (1 mg). The background fluorescence signal was found slightly higher in serum containing buffer. The lower aggregation peak at 705 nm suggested that the probe did interact with other proteins. However this nonspecific protein binding did not significantly inhibit the proteolysis, 40-fold activation was still observed with CyPEG-2.

We also compared fluorescence activation of CyPEG-2 with a commercially available reference peptide substrate, Z-Leu-Arg-MCA. While this coumarin-based substrate has a single copy of the peptide sequence (-Leu-Arg-), CyPEG probes incorporate four copies of the same. Z-Leu-Arg-MCA showed much lower activation (9-fold) as compared to CyPEG-2 (70-fold) under identical conditions. However, the activation was very rapid for this nonaggregated reference substrate, where fluorescence reached saturation in less than an hour. The aggregation of the probes did complicate the process of proteolysis. When incubating CyPEG-2 with different amounts of cathepsin S, a near linear dose response was observed in the first 60 min.

Selectivity Studies. The quenching efficiency and the activation profiles of CyPEG-1 and CyPEG-2 are similar but their aqueous solubility is dramatically different. Because CyPEG-2 has much higher aqueous solubility, this probe is better suited for biological applications. Selectivity studies with CyPEG-2 were performed under vendor-suggested optimized pH conditions using several cysteine proteinases, including cathepsin K, cathepsin L, and cathepsin S in 10 mM phosphate buffer solutions of pH 4.5, 5.5, and 6.5, respectively. DMSO (20%) was added to all the buffer solutions to improve the solubility of CyPEG-2 under acidic (pH 5.5 and 4.5) conditions. These cysteine proteases are known to be important in biological processes and have similar substrate selectivity. Interestingly, cathepsin L and cathepsin K did not show substantial activation

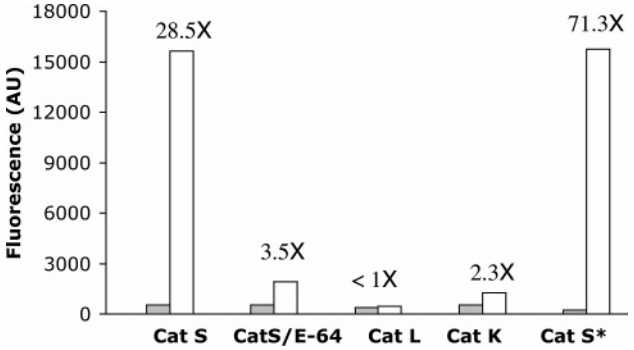

Figure 8. CyPEG-2 activation and selectivity under optimized pH conditions. Cathepsin S: pH 6.5, 10 mM phosphate buffer with 20% DMSO. Cathepsin S/E-64: pH 6.5, 10 mM phosphate buffer with 20% DMSO in the presence of E-64 protease inhibitor. Cathepsin L: pH 5.5, 10 mM phosphate buffer with 20% DMSO. Cathepsin K: pH 4.5, 10 mM phosphate buffer with 20% DMSO. Cathepsin S*: pH 6.5, 10 mM phosphate buffer. Probe activation (open bar) after 8 h at 810 nm as compared to the nonenzyme controls (solid bar).

of the probe (Figure 8). The Leu-Arg dipeptide cathepsin S substrate used in this study was previously reported to be partially but not completely selective to cathepsin S.[9,10] The selectivity observed for cathepsin S in the present study is higher than what was expected from the literature reports, a 2−3 fold difference.[9,10] The substrate selectivity changes observed in the MAP-based probes may be due to the substrate sequence and the aggregation associated with the multiple copies of the enzyme substrate. In our studies, we observed that the activity of cathepsin S remains unchanged in the presence of 20% or less of DMSO. Cathepsin K, also does not show much sensitivity toward DMSO. Cathepsin L, however, shows very diminished activity in the presence of DMSO. Also, factors such as the presence of dithiothritol and commercial source of the enzymes could be responsible for the selectivity observed in Figure 8.

Activation studies of CyPEG-2 with cathepsin S showed more than a 70-fold increase in fluorescence in pH 6.5 buffer without DMSO. Even in the presence of 20% DMSO, at pH 6.5, CyPEG-2 still showed a 28-fold increase in fluorescence (Figure 8). Importantly, the probe activation can be specifically inhibited by a synthetic cathepsin S inhibitor, E-64, supporting that the probe activation is protease dependent. The diminished activation in the presence of DMSO could originate from the ability of this organic solvent to break down the dye−dye aggregates. In a DMSO free buffer solution, the fluorochromes in the probe are expected to show an increased tendency to aggregate and hence lower background fluorescence (Figure 8).

CyTE-777 employed in the design of cathepsin activatable probes has its emission maxima above 800 nm. Thus, the fluorescence signal obtained from the activated probe is in the near-infrared (NIR) region, which is ideally suited for in vivo imaging.[15] One potential drawback of small, peptide-based molecular probes is their extremely rapid renal clearance and short plasma half-life. Pegylation of peptides and proteins generally improves their overall pharmacokinetics. Attaching small (350 Da) PEG chains show little or no effect in the pharmacokinetics of a large (17 kD) protein[13] as the short PEG chains cannot span the entire surface of the protein. However, the effect of multiple short PEG chains incorporated in a small peptide has been shown to be significant in the plasma half-life and renal clearance of small bioactive peptides[16] and peptide-based imaging agents,[17] as the short PEG chains can efficiently solvate the smaller surface area of a peptide.

The protease sensitive probes in this report were designed to be activated by cathepsin S (EC 3.4.22.27). Among 11 cysteine cathepsins present in the human genome, cathepsin S is unique because of its potential to be active at neutral pH in the extracellular matrix, suggesting its role in invasion.[18] High expression of cathepsin S has been found in lung alveolar macrophages,[19] brain tumor,[20] rheumatoid arthritis,[21] and atherosclerosis.[22] The enzymatic activity obtained by using these fluorescent probes potentially could be applied to clinical diagnosis.

Conclusion

Fluorescence quenching promoted by the MAP-based system was utilized for making an enzyme sensitive probe in which the existence of dye−dye aggregates could be abolished by addition of a protease. The design has two important features: (1) multivalency, which is required for the amplification of fluorescence, and (2) the ability to promote aggregation of the dyes that are otherwise in a free state in aqueous solutions. The core of the MAP system originates from a single amino acid residue and then extends into a branched structure in one direction where the dyes are attached to the PEG moiety and not to the peptide sequence. Therefore the influence of peptide sequence and its conformational features are less important in a MAP-based design of a probe. The MAP-based probes may prove to be a universal and robust design that can be exploited for development of fluorogenic probes for a variety of proteases via alteration of the enzyme substrate in the dendritic arms.

Experimental Section

Solid-Phase Peptide Synthesis. Probes—CyPEG-1, CyPEG-2, and CyPEG-3—were synthesized by solid-phase methods. Fifty milligrams of $Fmoc_4$-Lys_2-Lys-β-Ala Wang resin (100−200 mesh), purchased from Peptides International (Louisville, KY), was added into the 6 mL capacity single fritted reservoir (Biotage-Argonaut, Redwood City, CA) and shaken with 3.5 mL of dichloromethane (DCM) for 15 min. A tetrapeptide (β-Ala-Leu-Arg(Pbf)-β-Ala) was built on this solid support manually by using the following protocol. Fmoc deprotection: 2 cycles of 20 min each with 3.5 mL of 20% piperidine in *N*,*N*-dimethylformamide (DMF) followed by washing of the resin with DMF (4 × 3 mL). Amino acid coupling: 5 equiv (with respect to the loading level of the resin) of the fluorenylmethoxycarbonyl (Fmoc) protected amino acids (Novabiochem, San Diego, CA), 2-(1-*H*-benzotriazole-1-yl)-1,1,3,3-tetramethyluronium hexafluorophosphate (HBTU), and *N*-hydroxybezotriazole (HOBt) were dissolved in 3 mL of peptide synthesis grade DMF in a small glass beaker, and 100 μL of *N*,*N*-diisopropylethylamine (DIEPA) was added. The solution was allowed to stand for 15 min and was added to the resin in a single fritted reservoir. After tightly securing the reservoir, the suspension was shaken overnight. The resin was then washed four times with DMF and three times with DCM. All coupling reactions were monitored by the ninhydrin and chloranil tests[23] using a dry resin sample.

PEG Coupling. Five equivalents (80 mg) of Fmoc-15-amino-4,7,10,13-tetraoxapentadecanoic acid (NeoMPS, Strasbourg, France) and 110 mg of benzotriazole-1-yl-oxy-tris-pyrrolidino-phosphonium hexafluorophosphate (PyBOP) were dissolved in a 3 mL solution of 9:1 *N*-methyl-2-pyrrolidone (NMP)/DCM in a small glass beaker, and 60 μL of DIEPA was added. The solution was allowed to stand for 30 min and was added to the resin-bound tetrapeptide. The Fmoc group was deprotected as mentioned above. This protocol of PEG coupling and Fmoc deprotection was repeated once for CyPEG-2 and twice for CyPEG-3. All the couplings were monitored by the ninhydrin and chloranil tests using a dry resin sample.

Dye Conjugation. Following PEG coupling and Fmoc deprotection, the peptide resin was collected for further coupling of the NIR dye. Fifty milligrams of CyTE-777[11] (5 equiv) and 10 mg of HOBt were dissolved in 2 mL of anhydrous DMF and chilled to 0

°C. To this, 30 mg of *N*,*N*′-dicyclohexylcarbodiimide (DCC) was added and dissolved by gentle stirring. The solution was then warmed to the room temperature and allowed to stand for 60 min after which it was added to the resin-bound pegylated peptide.

Cleavage and Purification. Following dye conjugation, the resin was washed 5 times with DMF and 3 times with DCM and dried under vacuum. The dried resin sample (~50 mg) was treated with a 3 mL solution of 15:1 trifluoroacetic acid (TFA)/triisopropylsilane (TIS) for 2 h. The resin suspension was filtered into 30 mL of hexanes, and the solvents were removed in vacuo at 45 °C using a water aspirator. The dried sample was dissolved in 20 mL of 1:1 water/acetonitrile and lyophilized to obtain dry powder. Lyophilization was repeated twice. All the probes were purified by reversed phase−high performance liquid chromatography (RP-HPLC) using a Vydac preparative column (C18, 10 μm, 22 mm ID × 250 mm L, Hesperia, CA) on a Hitachi D-7000 HPLC system equipped with a Hitachi L-7100 pump and a Hitachi L-7455 diode array detector. HPLC conditions: buffer A−0.1% TFA in water, buffer B−0.1% TFA in acetonitrile; solvent gradient−0% B to 100% B in 50 min; flow rate−6 mL/min; UV detection−220 nm. The overall yield of synthesis was between 40 and 42% for all the three probes. The purity of the probes was confirmed by two divergent HPLC systems. System 1 was same as the above-described preparative HPLC, but an analytical C-18 reverse phase column (Vydac 218TP54, 5 μm, 4.6 mm ID × 250 mm) was used (Figure 3). The characterization data are summarized in Table 1. System 2 is described in the Supporting Information.

Enzymatic Studies. All the studies were performed in triplicate with 200 μL of the sample in a 96-well assay plate with clear bottom and lid (Corning Inc. NY). All the graphs indicate average values, and the error bars indicate standard deviation. Fluorescence measurements were obtained in a fully modular monochromator-based microplate detection system (Safire^2, Tecan, San Jose, CA). Enzymes and enzyme inhibitors were purchased from EMD Biosciences (San Diego, CA). Z-Leu-Arg-MCA (Benzyloxycarbonyl-L-leucyl-L-arginine 4-methylcoumaryl-7-amide) was purchased from Peptides International (Louisville, KY). Concentration of all the probes and CyTE-777 was adjusted to ~3 μM (based on the absorption spectra, O.D. of 0.4) using a solution of 20% dimethyl sulfoxide (DMSO) in 10 mM phosphate buffer, pH 7.4. For all the activation studies 0.55 nmol of probe and 0.16 nmol of enzyme (human recombinant cathepsin S, human liver cathepsin L, human recombinant cathepsin K) were mixed. The assays were performed under the optimized pH conditions as suggested by the vendor. Excitation and emission were set at 750 and 810 nm, respectively, with a bandwidth of 20 nm. The fluorescence was monitored for 9 h at 27 °C. Control experiments were performed simultaneously by replacing the enzyme with either 10 mM phosphate buffer or by adding E-64 protease inhibitor (2 nM) to the enzyme.

Acknowledgment. This research was supported in part by NIH P50-CA86355, RO1 CA99385, R21 CA114149, and the Donald W. Reynolds Foundation. S.A.H. was supported by NIH T32-CA79443.

Supporting Information Available: HPLC chromatograms of all three probes. This material is available free of charge via the Internet at http://pubs.acs.org.

References

(1) Tung, C. H. Fluorescent peptide probes for in vivo diagnostic imaging. *Biopolymers* **2004**, *76*, 391−403.
(2) Pham, W.; Choi, Y. D.; Weissleder, R.; Tung, C. H. Developing a peptide-based near-infrared molecular probe for protease sensing. *Bioconjugate Chem.* **2004**, *15*, 1403−1407.
(3) Weissleder, R.; Tung, C. H.; Mahmood, U.; Bogdanov, A. In vivo imaging of tumors with protease-activated near-infrared fluorescent probes. *Nature Biotechnol.* **1999**, *17*, 375−378.
(4) Josephson, L.; Kircher, M. F.; Mahmood, U.; Tang, Y.; Weissleder, R. Near-infrared fluorescent nanoparticles as combined MR/optical imaging probes. *Bioconjugate Chem.* **2002**, *13*, 554−560.
(5) Maeda, H. The enhanced permeability and retention (EPR) effect in tumor vasculature: The key role of tumor-selective macromolecular drug targeting. Adv. *Enzyme Regul.* **2001**, *41*, 189−207.
(6) Merrifield, R. B. Solid-phase peptide synthesis. 1. Synthesis of a tetrapeptide. *J. Am. Chem. Soc.* **1963**, *85*, 2149−2154.
(7) Tam, J. P. Synthetic peptide vaccine design − synthesis and properties of a high-density multiple antigenic peptide system. *Proc. Natl. Acad. Sci. U.S.A.* **1988**, *85*, 5409−5413.
(8) Crespo, L.; Sanclimens, G.; Pons, M.; Giralt, E.; Royo, M.; Albericio, F. Peptide and amide bond-containing dendrimers. *Chem. Rev.* **2005**, *105*, 1663−1681.
(9) Bromme, D.; Okamoto, K.; Wang, B. B.; Biroc, S. Human cathepsin O-2, a matrix protein-degrading cysteine protease expressed in osteoclasts − functional expression of human cathepsin O-2 in spodoptera frugiperda and characterization of the enzyme. *J. Biol. Chem.* **1996**, *271*, 2126−2132.
(10) Bossard, M. J.; Tomaszek, T. A.; Thompson, S. K.; Amegadzie, B. Y.; Hanning, C. R.; Jones, C.; Kurdyla, J. T.; McNulty, D. E.; Drake, F. H.; Gowen, M.; Levy, M. A. Proteolytic activity of human osteoclast cathepsin K − expression, purification, activation, and substrate identification. *J. Biol. Chem.* **1996**, *271*, 12517−12524.
(11) Hilderbrand, S. A.; Kelly, K. A.; Weissleder, R.; Tung, C. H. Monofunctional near-infrared fluorochromes for imaging applications. *Bioconjugate Chem.* **2005**, *16*, 1275−1281
(12) Caliceti, P.; Veronese, F. M. Pharmacokinetic and biodistribution properties of poly(ethylene glycol)-protein conjugates. *Adv. Drug Deliv. Rev.* **2003**, *55*, 1261−1277.
(13) Packard, B. Z.; Toptygin, D. D.; Komoriya, A.; Brand L. Design of profluorescent protease substrates guided by exciton theory. *Methods Enzymol.* **1997**, *278*, 15−23.
(14) Johansson, M. K.; Cook, R. M. Intramolecular dimers: A new design strategy for fluorescence-quenched probes. *Chem. Eur. J.* **2003**, *9*, 3466−3471.
(15) Weissleder, R.; Ntziachristos, V. shedding light onto live molecular targets. *Nat. Med.* **2003**, *9*, 123−128.
(16) Lee, S. H.; Lee S.; Youn, Y. S.; Na, D. H.; Chae, S Y.; Byun, Y.; Lee, K. C. Synthesis, characterization, and pharmacokinetic studies of PEGylated glucagon-like peptide-1. *Bioconjugate Chem.* **2005**, *16*, 377−382.
(17) Chen, X. Y.; Park, R.; Hou, Y. P.; Khankaldyyan, V.; Gonzales-Gomez, I.; Bading, J. R.; Laug, W. E.; Conti, P. S. MicroPET imaging of brain tumor angiogenesis with F-18-labeled PEGylated RGD peptide. *Eur. J. Nucl. Med. Mol. Imaging* **2004**, *31*, 1081−1089.
(18) Turk, V.; Kos, J.; Turk, B. Cysteine cathepsins (proteases) − on the main stage of cancer? *Cancer Cell* **2004**, *5*, 409−410.
(19) Kos, J.; Sekirnik, A.; Kopitar, G.; Cimerman, N.; Kayser, K.; Stremmer, A.; Fiehn, W.; Werle, B. Cathepsin S in tumors, regional lymp nodes, and sera of patients with lung cancer: Relation to prognosis. *Br. J. Cancer* **2001**, *85*, 1193−1200.
(20) Flannery, T.; Gibson, D.; Mirakhur, M.; McQuaid, S.; Greenan, C.; Trimble, A.; Walker B.; McCormick, D.; Johnston, P. G. The clinical significance of cathepsin S expression in human astrocytomas. *Am. J. Pathol.* **2003**, *163*, 175−182.
(21) Yasuda, Y.; Kaleta, J.; Bromme, D. The role of cathepsins in osteoporosis and arthritis: Rationale for the design of new therapeutics. *Adv. Drug Deliv. Rev.* **2005**, *57*, 973−993.
(22) Liu, J.; Sukhova, G. K.; Sun, J. S.; Xu, W. H.; Libby, P.; Shi, G. P. Lysosomal cysteine proteases in atherosclerosis. *Arterioscler. Thromb. Vasc. Biol.* **2004**, *24*, 1359−1366.
(23) Kay, C.; Lorthioir, O. E.; Parr, N. J.; Congreve, M.; McKeown, S. C.; Scicinski, J. J.; Ley, S. V. Solid-phase reaction monitoring − chemical derivatization and off-bead analysis. *Biotechnol. Bioeng.* **2000**, *71*, 110−118.

JM051001A